Microwave-hydrothermal Synthesis and Luminescence Properties of CeF_3

Chunni Tang[1*], Jun Fan[2], Enzhou Liu[2] and Wenqian Hou[2]

[1] Department of Chemical Engineering, Shaanxi Institute of Technology, 710300 Xi'an, China

[2] School of Chemical Engineering, Northwest University, 710069 Xi'an, China

[*] Corresponding author: tcn2007@126.com

Abstract. Luminescent material CeF_3 was synthesized by a facile and effective microwave-hydrothermal method. The products were characterized by X-ray diffraction (XRD), transmission electron microscopy (TEM), field-emission scanning electron microscopy (FESEM), BET method and photoluminescence (PL). The results indicated that specific morphology and size of product could be controlled by changing fluorine sources and reaction temperatures. Varing fluorine sources from NH_4F to KBF_4, hollow CeF_3 nanocrystals or multidimensional disk-like CeF_3 microcrystals could be obtained respectively. With increasing reaction temperature, the surface areas of samples decreased and sizes and crystalline increased. PL spectra showed that the CeF_3 samples exhibited emissions of Ce^{3+} (5d-4f) and they could achieve not only downconvertion luminescence but also upconvertion luminescence. The luminescence properties were related to not only size and crystalline but also shape. Furthermore, the mechanism of luminescence of the CeF_3 samples was proposed and the upconversion luminescence could be deduced to the multi-photon simultaneous absorption luminescence.

1. Introduction

In recent years, great effort has been devoted to the synthesis and property of CeF_3 micro- and nano-crystals. Due to its high density, fast response and high radiation resistance, it is considered as one of the most promising scintillators for the next generation experiments in high-energy physics[1]; owing to its lower phonon-energy and low rate of fluorescence quenching, it is also an important fluorescent host material[2]; because of its layered structures, CeF_3 is also a good solid lubricant[3]. So far, various methods, including hydrothermal[4] or solvothermal[5] process, polyol methods[6], microwave irradiation[7], ionic liquid methods[8], reverse micelles or microemulsions[9] have been developed to synthesize CeF_3 with specific shape and unique properties such as nanoparticles[6], nanocrystals[10], nanoplates[11], nanowires[12], nanocages[13], nanorings[13], nanococoons [13], circular hollow disks[13], disk-like[14] and flower-like nanostructures[7]. However, it is still a challenge to fabricate some novel structures of CeF_3 with well-controllable morphology and size and investigate the effects of morphology and size on photoluminescent properties.

Furthermore, CeF_3 was rarely considered as an upconversion luminescent material (ULM) in the past years because energy levels of Ce^{3+} are too simple and lack of corresponding metastable energy levels in visible region or near infrared region. Recently, it was demonstrated that the upconversion luminescence of Ce^{3+} doped in different host materials excited by simultaneous absorption of three

infrared photons using the fem tosecond laser irradiation[15,16]. This discovery suggests that CeF_3 could be a good candidate for ULM. Therefore, it is also a challenge to investigate the properties and mechanism of upconversion luminescence of CeF_3.

In this paper, we reported a facile rapid microwave-hydrothermal method to prepare CeF_3. The influences of fluorine sources and reaction temperatures on the morphology and size of the final products were studied. In addition, the photoluminescent (PL) properties, especially upconversion luminescence of as-prepared samples with different shape and size were also investigated.

2. Experimental Section

2.1. Sample preparation

The luminescent material CeF_3 was prepared by a microwave-hydrothermal method. In a typical procedure, 1 mmol $Ce(NO_3)_3 \cdot 6H_2O$ was dissolved in 15 mL of distilled water, then 15 mL of distilled water containing 9 mmol NH_4F was dripped into the solution under stirring. The suspension was transferred into a teflon lined vessel and experienced a microwave treatment at appropriate temperatures for 30 min. Finally, the products were collected by centrifugation, washed and dried. The samples synthesized at appropriate temperatures of 120, 180 and 220 ºC were denoted as S1, S2 and S3, respectively. S4 employed a similar synthetic procedure in 180 ºC using KBF_4 as fluorine source.

2.2. Characterization

X-ray diffraction patterns (XRD) of the samples were obtained on a Bruker D8 advance diffractometer. Transmission electron microscope (TEM) was recorded on a JEM-100SX electron microscope. Field-emission scanning electron microscope (FESEM) images were taken on a JSM-6390A electron microscope. Nitrogen desorption curves were obtained using a quantachrome NOVA 2000e apparatus. The room temperature photoluminescence (PL) spectrums were measured on a Hitachi F-7000 fluorescence spectrophotometer.

3. Results and Discussion

3.1. Microstructure analysis

Fig. 1 shows the XRD patterns of the as-synthesized CeF_3 samples. The high and sharp peaks in the patterns indicate that all of the samples are well crystallized. The characteristic diffraction peaks of the hexagonal phase CeF_3 can be observed, which are in good agreement with those in the standard JCPDS file No.08-0045. With increasing temperatures from 120 ºC to 220 ºC (S1~S3 in Fig.1), the XRD patterns of CeF_3 (fluorine source: NH_4F) become narrower and narrower, suggesting a gradually increased tendency of crystalline and size according to the Scherrer equation ($D= k\lambda/\beta\cos\theta$). Compared with S2 (fluorine source: NH_4F), the peaks in the pattern of S4 (fluorine source: KBF_4) appear to be noticeably sharper, corresponding to dramaticlly larger average grain size. In addition, the relative intensities of diffraction peaks of S4 are approximately changed, which indicate the orientation of crystal growth can be influenced by different fluorine source, and the products may exhibit different shapes. Based on the XRD analysis, we can conclude that temperatures and fluorine sources play important factors in controlling the size and the orientation of crystal growth.

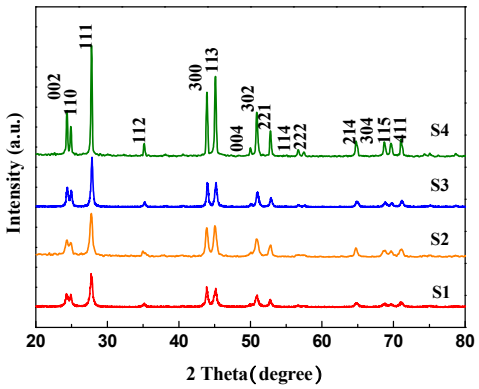

Fig. 1. XRD patterns of CeF_3 S1~3 (fluorine source: NH_4F) obtained at different temperatures (120, 180, 220 ºC) and S4 (fluorine source: KBF_4) obtained at 180 ºC.

The morphology of the as-prepared CeF_3 is investigated in Fig. 2. Seen in the TEM images of CeF_3 (Fig. 2. (A, B and C)), all of the CeF_3 samples (S1~S3) synthesised with KBF_4 as fluorine source are nano-hollow sphere-like or rod-like particles, but the size and morphology of samples obtained at different temperatures are different. When the temperature is 120 ºC, the sphere-like nanoparticles have a diameter of about 20~30 nm, while rod-like nanoparticles have a length of 20~30 nm and a diameter of about 15 nm. As the temperature increases to 180 ºC, some little hollow-particles have interlocked together to form bigger particles with multiple inside cavities. Upon further increasing the temperature to 220 ºC, the size of the nanoplates become bigger and bigger. The diameters of sphere-like nanoparticles are growth to 40~60 nm and the length and diameter of rod-like nanoparticles are growth to about 80 nm and 30 nm respectively. Meanwhile, the sizes of the inside cavities also increase

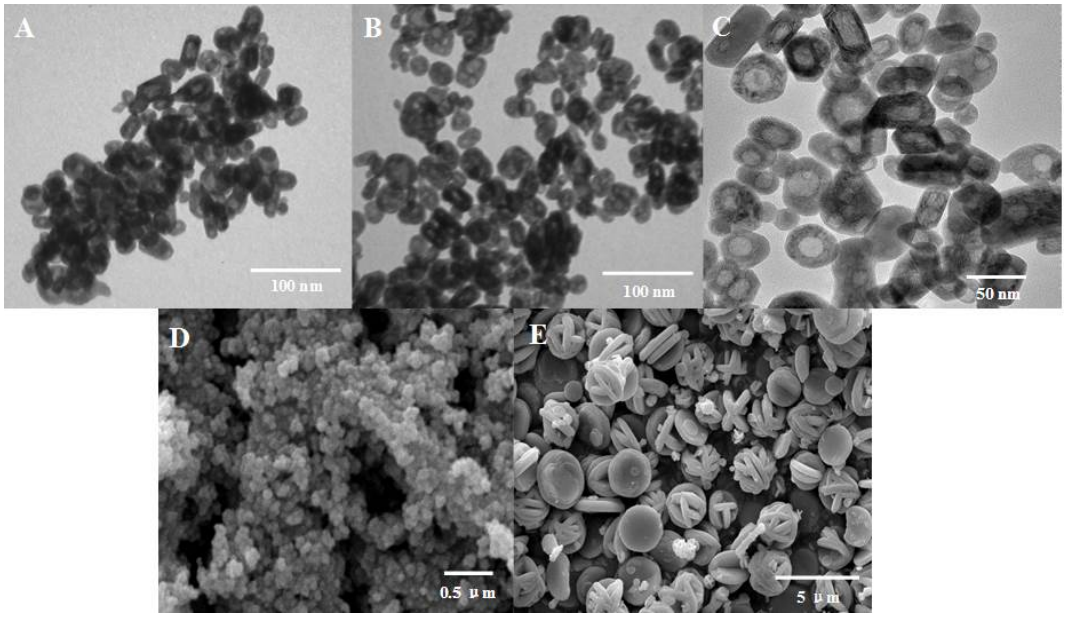

Fig. 2. TEM images of CeF_3 samples: (A) S1, (B) S2, (C) S3, FESEM images of CeF_3 samples: (D) S2, (E) S4.

compared with which are in S1 and S2. Seen in the FESEM images of CeF_3 (Fig. 2. (D and E)), the morphologys of the samples are obviously different when using different fluorine source. S2 are sphere-like or rod-like nanoparticles, while S4 are uniform multidimensional disk-like or flower-like particles and the average diameters and thickness of the plates are 2.5 μm and 300 nm respectively, indicating the morphologies and particle sizes of CeF_3 are effected by fluorine sources.

Nitrogen adsorption-desorption isotherms of CeF_3 were shown in Fig. 3. CeF_3 S1~S3 yield isotherms (type IV) with H_3-type hysteresis, which indicate that some crack-like mesopores (2 nm ~ 50 nm) exist in samples. With increasing temperatures from 120 ºC to 220 ºC (S1~S3 in Fig. 3), the Brunauer-Emmett-Teller (BET) surface areas of CeF_3 become smaller and smaller (S1: 46.166 m^2/g, S2: 32.961 m^2/g, S3: 27.032 m^2/g, respectively), suggesting a gradually increased tendency of the crystallite size. CeF_3 S4 prepared with KBF_4 as fluorine source also yields a type IV isotherm with H_3-type hysteresis, but its surface area is low to 2.842 m^2/g, which results from the large size and smooth surface of S4. The results confirm that BET surface areas of CeF_3 are not only dependent on reaction temperatures but also on the fluorine sources.

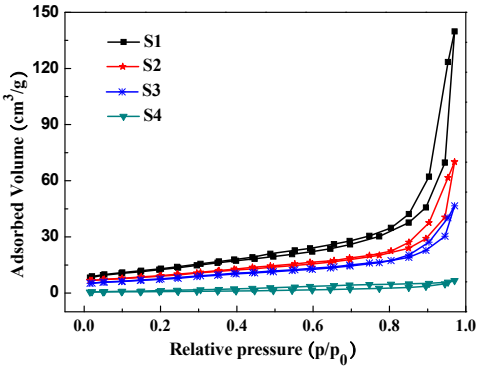

Fig. 3. Nitrogen adsorption-desorption isotherms of CeF_3 S1~4.

3.2. Luminescence properties

3.2.1. Downconversion luminescence properties

The three-dimensional downconversion luminescence scan spectrum, the excitation and emission spectra of CeF_3 S2 were measured (See Fig. 4). It can be seen clearly that CeF_3 samples can convert MUV (200 nm ~ 310 nm) into NUV (285 nm ~ 380 nm), and two emission peaks at 304 nm and 324 nm are observed under the excitation of 260 nm and 280 nm at room temperature, which is probably assigned to Ce^{3+} electrons' transfer between the different sub-levels of 5d excited states split by the crystal field [17, 18] and the 4f ground state ($^2F_{5/2}$ and $^2F_{7/2}$). The phenomena demonstrate obvious properties of broad-band absorption and emission, which is in consistence with most references [19].

Fig. 5 shows the emission spectra of the CeF_3 samples S1~4. With an increase in temperature from 120 ºC to 220 ºC (S1~S3 in Fig. 5), the emission spectra are similar in shapes and positions, but the intensities of the emission light are increasing. These results may be related to the semblable morphologies with only slightly differences in crystalline and size of CeF_3. Analyzed from the XRD、TEM and BET, samples S1~S3 have similar morphologies, and their specific surface areas decrease with sizes and crystalline increasing in sequence. These lead to a decrescent probability that CeF_3 could be oxidized or formed defect on their surface, and in consequence the luminescence intensities of samples enhance in sequence. Meantime, with the increasing temperature (S1~S3 in Fig.5), the emission peaks have slightly blue shifts. These results may be related to the variations of 5d excited state of Ce^{3+} in different samples. For Ce^{3+}, the 6S electronic shell has no electron, so its 5d excited electronic configuration of Ce^{3+} is not shielded from the surroundings and is very sensitive to the change surrounding Ce^{3+} ions at or near the surface[20], which may ascend when the grain size becomes bigger and lead to a blue shift in the emission spectra.

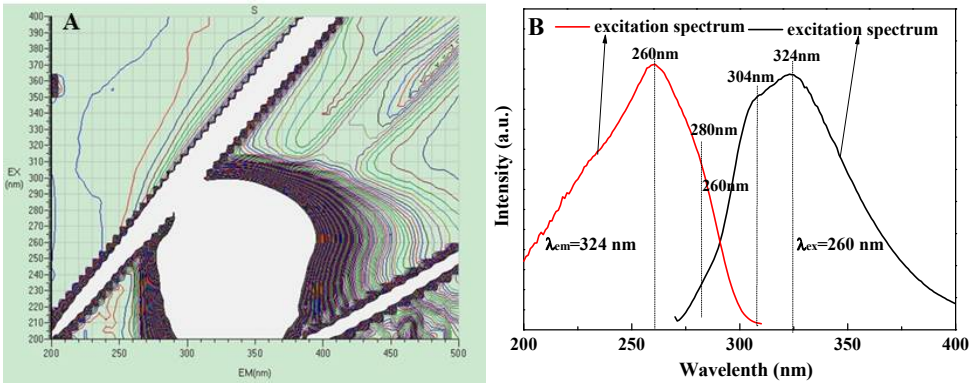

Fig. 4. (A) The three-dimensional downconversion luminescence scan spectrum of CeF_3 S2; (B) Downconvertion excitation spectrum of CeF_3 S2 and the emission spectrum.

However, using different fluorine source, there are clear differences between the emission spectrum of CeF_3 S4 (fluorine source: KBF_4) and that of CeF_3 S2 (fluorine source: NH_4F). The intensities of the emission light present dramatically descent and the emission peaks have blue shifts. It can be illustrated that the emission spectrum is related to not only size and crystalline but also shape and surface areas. Compared to CeF_3 S2, the size of S4 increases by two orders of magnitude and reach to micron, the surface area of S4 decreases by one order of magnitude, and the shape becomes disk-like or flower-like.

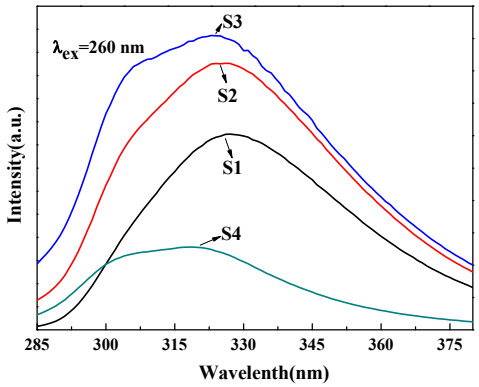

Fig. 5. Downconvertion emission spectra of CeF_3 S1~S4 (the monitoring wave-length is 260 nm).

3.2.2. Upconversion luminescence properties

The three-dimensional upconvertion luminescence scan spectrum of CeF_3 was measured (Fig. 6(A)). It can be seen clearly that the visible light (420 nm ~ 600 nm) and near-infrared light (750 nm ~ and 870 nm) can be converted into ultraviolet (UV) light (285 nm–380 nm) by CeF_3. Fig. 6(B) and (C) shows the upconversion luminescence emission and excitation spectra of CeF_3 S2. Using the monitoring wavelength at 324 nm, two visible light excitation peaks at 524 nm and 554 nm and two near-infrared light excitation peaks at 780 nm and 850 nm are found in the excitation spectra of CeF_3 (Fig. 6 (B)). Using the monitoring wavelengths at 524 nm, 554 nm 780 nm and 850nm respectively, two UV emission peaks at 304nm and 324nm are detected in the emission

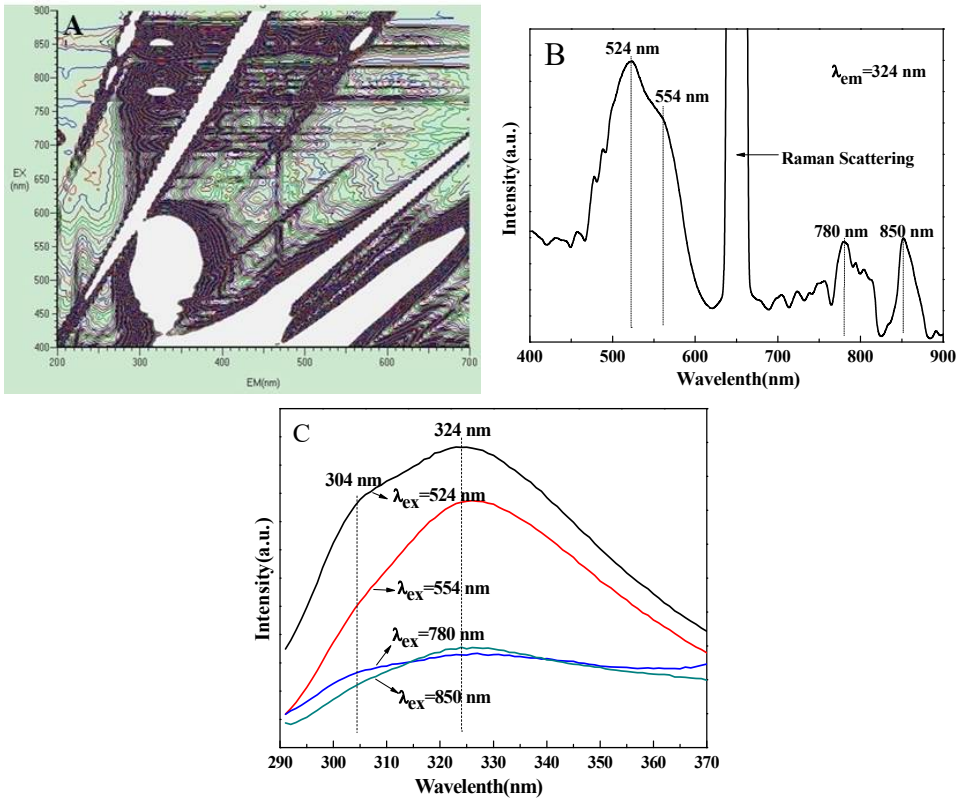

Fig. 6. (A) The three-dimensional upconversion luminescence scan spectrum of CeF3 S2; (B) Upconvertion excitation of CeF_3 S2; (C) emission spectra of CeF_3 S2.

spectrum of CeF_3 (Fig. 6 (C)). Meanwhile, with increasing in wavelengths of excitation light, the intensities of emission lights are decreasing. Seen from Fig. 7, the effects of different CeF_3 samples (S1~S4) on the upconvertion emission spectra are similar to that of the downconvertion emission spectra (Fig. 5), indicating that the variation tendency also due to the change of size, crystalline and shape of samples.

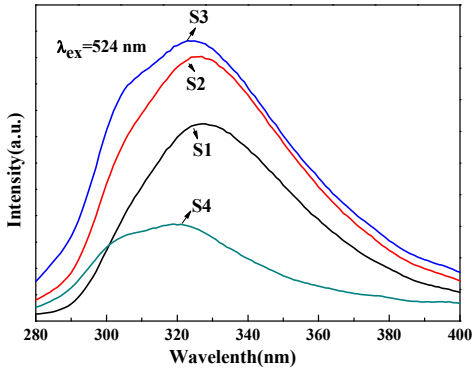

Fig. 7. Upconvertion emission spectra of CeF_3 S1~S4 (the monitoring wave-length is 524 nm).

3.2.3. Mechanism of luminescence

In Downconvertion excitation spectrum of CeF_3 S3 (Fig. 4), the main emission peaks of CeF_3 are about at 304 nm and 324 nm, which can ascribe to electron transitions from the lowest split energy level of 5d to $^2F_{5/2}$ and $^2F_{7/2}$ in Ce^{3+} respectively. Meanwhile, the main excitation peaks are about at 260 nm and 280 nm, which is attributed to electron' transitions from the $^2F_{5/2}$ ground state to different sub-levels of the 5d states in Ce^{3+}split by the crystal field [21].

It is apparent that the emission spectra of upconversion luminescence are similar to that of the down-conversion luminescence in shapes and positions and variation tendencies, which indicate that the mechanism of upconversion luminescence of CeF_3 can also be assigned to the same Ce^{3+} electronic radiative transition (5d-4f). The exciting energy of 260 nm is almost twice and three times as much as the excitation light of 524 nm and 780 nm respectively, and the exciting energy of 280 nm is twice and three times as much as the excitation light of 554 nm and 850 nm respectively. Therefore, the upconversion of visible light and near-infrared light are probably dominated by two-photon or three-photon excitation process. However, because there is not intermediate energy levels between 5d and 4f levels of Ce^{3+}[22], the mechanism of up-conversion luminescence of CeF_3 could not be the usual mechanisms of up-conversion luminescence including ESA (Excited State Absorption), ET (Energy Transfer) or PA (Photo Avalanche), all of which need intermediate levels. Hence, it may be deduced to multi-photon simultaneous absorption[23]. This mechanism could be considered that more than one photon are absorbed at the same time, which results in direct electron excitation from an initial state to a final state.

The mechanism of luminescence was proposed in figure 8. First, the electron located on the ground state ($^2F_{5/2}$) simultaneously absorb one 260 nm photon (4.77 eV) or two 524 nm photons (2.37 eV) or three 780 nm photons (1.59 eV) and transfer to the excited 5D state (4.77 eV), and it absorb one 280 nm photon (4.43 eV) or two 554 nm photons (2.24 eV) or three 850 nm photons (1.46 eV) and transfer to the excited 5D state (4.43 eV). Then, electron nonradiatively relax to the lowest 5D state (4.08 eV). Finally, the transitions from the lowest 5D state to the ground state ($^2F_{5/2}$) or the state ($^2F_{7/2}$) result in the emissions at 304 nm and 324 nm.

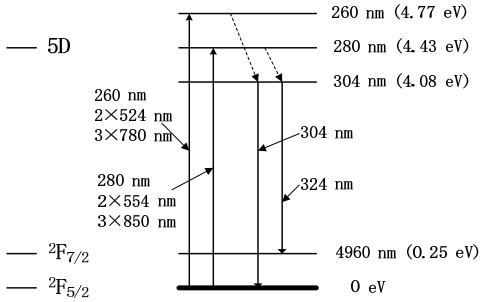

Fig. 8. Upconversion luminescence process of the CeF_3 sample.

4. Conclusion

In summary, hexagonal phase CeF_3 with good crystallinity have been successfully fabricated through a facile and effective microwave-hydrothermal method. Varing fluorine source from NH_4F to KBF_4, hollow CeF_3 nanocrystals or multidimensional disk-like CeF_3 microcrystals could be obtained respectively. With increasing reaction temperature, the surface areas of samples decreased and sizes and crystalline increased. PL spectra show that the CeF_3 samples exhibit emissions of Ce^{3+} (5d→4f) and they can achieve not only downconvertion luminescence but also upconvertion luminescence. The luminescence properties are related to not only size and crystalline but also shape. Furthermore, the mechanism of luminescence of the CeF_3 samples is proposed and the upconversion luminescence could be deduced to the multi-photon simultaneous absorption luminescence. The as-synthesized luminescent product may have some potential applications in the areas of light display.

This work supported by the Scientific Reaearch Program Funded by Shaanxi Provincial Education Department (Program No. 17JK0064), and the Research and Development Project of Shaanxi Institute of Technology (Gfy18-xx).

References

[1] Y. Pei, X.F. Chen, D.M. Yao, G.H. Ren, Radiat. Meas. **42**, 1351-1354(2007)
[2] Z.L. Wang , Z.W. Quan , P.Y. Jia , C.K. Lin , Y. Luo, Y. Chen , J. Fang , W. Zhou , C.J. O'Connor , and J. Lin, Chem. Mater. **18**, 2030-2037(2006)

[3] L.B. Wang, M. Zhang, X.B. Wang, W.M. Liu, Mater. Res. Bull. **43**, 2220-2227 (2008)
[4] Y. Liu, Y.B. Zhao, H.J. Luo, J. Nanoparticle. Res. **13**, 2904-2910 (2011)
[5] X.S. Qu, H.K. Yang, J.W. Chung, J. Solid State Chem. **184**, 246-251(2011)
[6] S. Eiden-Assmann, G. Maret, Mater. Res. Bull. **39**, 21-24 (2004)
[7] L. Ma, W.X. Chen, X.Y. Xu, L.M. Xu, X.M. Ning, Mater. Lett. **64,** 1559-1561 (2010)
[8] V. Bartuneˇk, J. Rak, V. Kra´l, J. Fluorine Chem. **132**, 298-301 (2011)
[9] H. Lian, M. Zhang, J. Liu, Z. Ye, J. Yan, C. Shi, Chem. Phys. Lett**. 395**, 362-365(2004)
[10] L. Zhu, Q. Li, X.D. Liu, J.Y. Li, Y.F. Zhang, J. Meng, and X.Q. Cao, J. Phys. Chem. C, **111**, 5898-5903(2007).
[11] C.X. Li , X.M. Liu , P.P. Yang , C.M. Zhang , H.Z. Lian , and J. Lin, Phys. Chem. C, **112,** 2904-2910 (2008)
[12] Z.Y. Wang , Z.B. Zhao, and J.S. Qiu, Chem. Mater. **19**, 3364-3366(2007)
[13] Q. Wu, Y. Chen, P. Xiao, J. Phys. Chem. C, **11**, 9604-9609(2008)
[14] L. Ma, W.X. Chen, Z.D. Xu, Mater. Lett. **62**, 2596 -2599 (2008)
[15] C. Wang, M.Y. Peng, L.Y. Yang, X. Hu, N. Da, D.P. Chen, C.S. Zhu, J.R. Qiu, J. Rare Earth. 2006, **24,** 754-756 (2006)
[16] Y.J. Dong, J. Xu, G.Q. Zhou, G.J. Zhao, M.Y. Jie, L.Y. Yang, L.B. Su, J.R. Qiu, W.W. Feng, L.H. Lin, Opt. Express. **14**, 1899-1904 (2006)
[17] G.J. Zhao, L.H. Zhang, X.M. He, H.Y. H.J. Li, J.Xu, X.H. Zeng, Chin. Phys. Soc. **54**, 612-616(2005)
[18] M.J. Weber, J. Appl.Phys. **44**, 3205-3208(1973).
[19] K. Klier, P.Novak, A.C. Miller, J.A. Spirko, M.K. Hatalis, J. Phys. Chem. Solid. **70**, 1302-1311(2009)
[20] L. Yu, H. Song, Z. Liu, L. Yang, S. Lu, and Z. Zheng, J. Phys. Chem. B, **109**, 11450-11455(2005)
[21] X. Qu, H.K.Yang, J.W. Chung, B.K. Moon, B.C. Choi, J.H. Jeong, J. Solid State Chem. **184**, 246-251(2010)
[22] D.B. Hamal, K.J. Klabunde. J. Colloid Interf. Sci. **311**, 514-522(2007)
[23] C. Wang, L.Y. Yang, Y.J. Dong, J. Xu, D.P. Chen, J.R. Qiu, J. Synth. Cryst. **36**, 526-530 (2007)